发 光 学 报
CHINESE JOURNAL OF LUMINESCENCE

Article ID: 1000-7032(XXXX)XX-0001-10

Efficient Perovskite Quantum Dots Light-Emitting Diodes: Challenges and Optimization

LI Mengjiao, WANG Ye, WANG Yakun*, LIAO Liangsheng

(*Key Laboratory for Carbon-Based Functional Materials & Devices, Institute of Functional Nano & Soft Materials, Soochow University, Suzhou*215123, *China.*)

* *Corresponding Author, E-mail: wangyakun@suda. edu. cn*

Abstract: Perovskite quantum dot light-emitting diodes (Pe-QLEDs) have shown immense application potential in display and lighting fields due to their narrow full-width at half maximum (FWHM) and high photoluminescence quantum yield (PLQY). Despite significant advancements in their performance, challenges such as defects and ion migration still hinder their long-term stability and operational efficiency. To address these issues, various optimization strategies, including ligand engineering, interface passivation, and self-assembly strategy, are being actively researched. This review focuses on the synthesis methods, challenges and optimization of perovskite quantum dots, which are critical for the commercialization and large-scale production of high-performance and stable Pe-QLEDs.

Key words: Pe-QLEDs; photoluminescence; defects; ion migration

CLC number: Document **Document code**: **DOI**: 10. 37188/CJL. 20240276

高效钙钛矿量子点发光二极管:挑战和优化

李梦娇, 王晔, 王亚坤*, 廖良生

(苏州大学,功能纳米与软物质研究院,碳基功能材料与器件重点实验室,江苏 苏州 215123)

摘要: 钙钛矿量子点发光二极管(Pe-QLEDs)由于其窄的半峰宽和高光致发光量子产率(PLQY)在显示和照明领域展现出巨大的应用潜力。尽管其性能已取得显著进展,但依然面临缺陷、离子迁移等诸多挑战,影响了其长期稳定性和操作效率。为了解决这些问题,配体工程、界面钝化、自组装策略等优化手段正在被广泛研究。本综述主要从钙钛矿量子点的合成、挑战和优化三个方面进行描述,这对实现高性能和稳定PeQLEDs的商业化和大规模生产至关重要。

关 键 词: 钙钛矿量子点发光二极管(Pe-QLEDs); 光致发光; 缺陷; 离子迁移

1 Introduction

The 2023 Nobel Prize in Chemistry was awarded to quantum dots[1-2] (QDs) pioneers Moungi Bawendi, Louis Brus, and Alexei Ekimov for their groundbreaking work on the discovery and synthesis of QDs. The discovery of QDs dates back to the 1980s. Alexei Ekimov[3] first demonstrated size-dependent quantum effects in colored glass. Around the same time, Louis Brus[4] provided evidence of these effects in particles suspended in fluid. In 1993, Moungi Bawendi[5] revolutionized the synthesis of QDs by developing a method to produce monodis-

收稿日期: XXXX-XX-XX; **修订日期**: XXXX-XX-XX
基金项目: 国家自然科学基金(62205230, 62175171, 62474119)
This work was supported by the National Natural Science Foundation of China (NSFC) (62205230, 62175171 and 62474119)

perse nanocrystals with precise size control. Since then, semiconductor QDs research has entered a new era, and the number of studies has increased exponentially.

When electrons are confined to a region comparable to their de Broglie wavelength, quantum confinement[6] occurs, which imparts many unique properties to QDs. High-quality QD samples exhibit narrow emission linewidths (20-80 meV), with the full width at half maximum[7] (FWHM) being measured, and near-unity photoluminescence quantum yield[8] (PLQY), making QDs one of the most promising materials for commercial televisions and displays. Of particular note, quantum dot light-emitting diodes[9] (QLEDs) have shown exceptional performance in wide-color-gamut displays, which places them as a frontrunner for advanced display technologies of the future.

Various types of QDs have been extensively studied, including II-VI QDs, III-V QDs, and lead halide perovskite QDs (PQDs)[2,10]. The first and most mature QDs are II-VI QDs, particularly CdE (E = S, Se, Te), which are renowned for their near-perfect PLQY and excellent stability. However, due to environmental and health concerns, Cd has been restricted in many consumer electronics. In contrast, PQDs are distinguished among Cd-free QDs due to their exceptional optical properties across red, green, and blue emissions.

In addition, since the pioneering work of Friend et al. in 2014, which demonstrated perovskite light-emitting diodes[11-12] (Pe-LEDs) emitting light at room temperature through optimized design of the luminescent layer, improvements in carrier injection and exciton recombination in the luminescent layer have led to significant advancements in perovskite QLEDs (Pe-QLEDs) devices. Within just a few years, through optimizations of QDs materials and device structures, Pe-QLEDs have achieved EQE exceeding 20% for both red and green devices, while blue QLEDs have reached an EQE of 18%. This rapid progress highlights the competitive advantage of PQDs in the display and lighting industries, signaling a strong momentum for future developments.

2 Optical Properties of PQDs

The typical structure of PQDs follows the ABX_3 configuration, where A typically refers to Cs^+, $CH_3NH_3^+$ (MA^+), or $CH(NH_2)_2^+$ (FA^+); B represents the divalent lead cation (Pb^{2+}); and X denotes a halogen ion (Cl^-, Br^-, or I^-). This flexible structure supports the distinctive optical and electronic properties of PQDs. As alternatives to conventional QDs, PQDs possess extremely low formation energy[13] and defect tolerance, as shown in Fig. 1(f). These characteristics give PQDs outstanding optical qualities, including nearly uniform high PLQY, narrow emission bandwidths, adjustable wavelengths across the visible spectrum, and adaptability to flexible and stretchable electronic devices. Most importantly, the phase characteristics of PQDs, specifically their morphology and shape, are effectively preserved even after the anion exchange reaction, as shown in Fig. 1 (a) and (e). These PQDs exhibit a tunable spectral range[14] by adjusting the halide composition and quantum confinement effects, as shown in Fig. 1(b) and (d), bringing Pe-QLEDs devices closer to commercialization. Additionally, they can also achieve a broader color gamut than the NTSC standard[14], as shown in Fig. 1(c). Notably, extensive research has demonstrated that QLEDs devices perform exceptionally well in wide color gamut displays, making them strong candidates for next-generation displays[15], as shown in Fig. 1(g) and (h).

3 Challenges

During the synthesis of PQDs, unfavorable reaction conditions (such as temperature, time, and reactant concentration) may lead to incomplete reactions of the reactants, resulting in unreacted materials or intermediate products, which introduce defects[17]. To intentionally introduce varying defect densities, Jun-Zhi Ye et al. employed a low-polarity antisolvent, methyl acetate, during the purification process of synthesized $CsPbBr_3$, $CsPbBr_xI_{3-x}$, and $CsPbI_3$ QDs[18] as shown in Fig. 2(a). As shown in Figure 2c, deep-level defects are nearly nonexistent in lead halide perovskite (LHP) QDs due to their high forma-

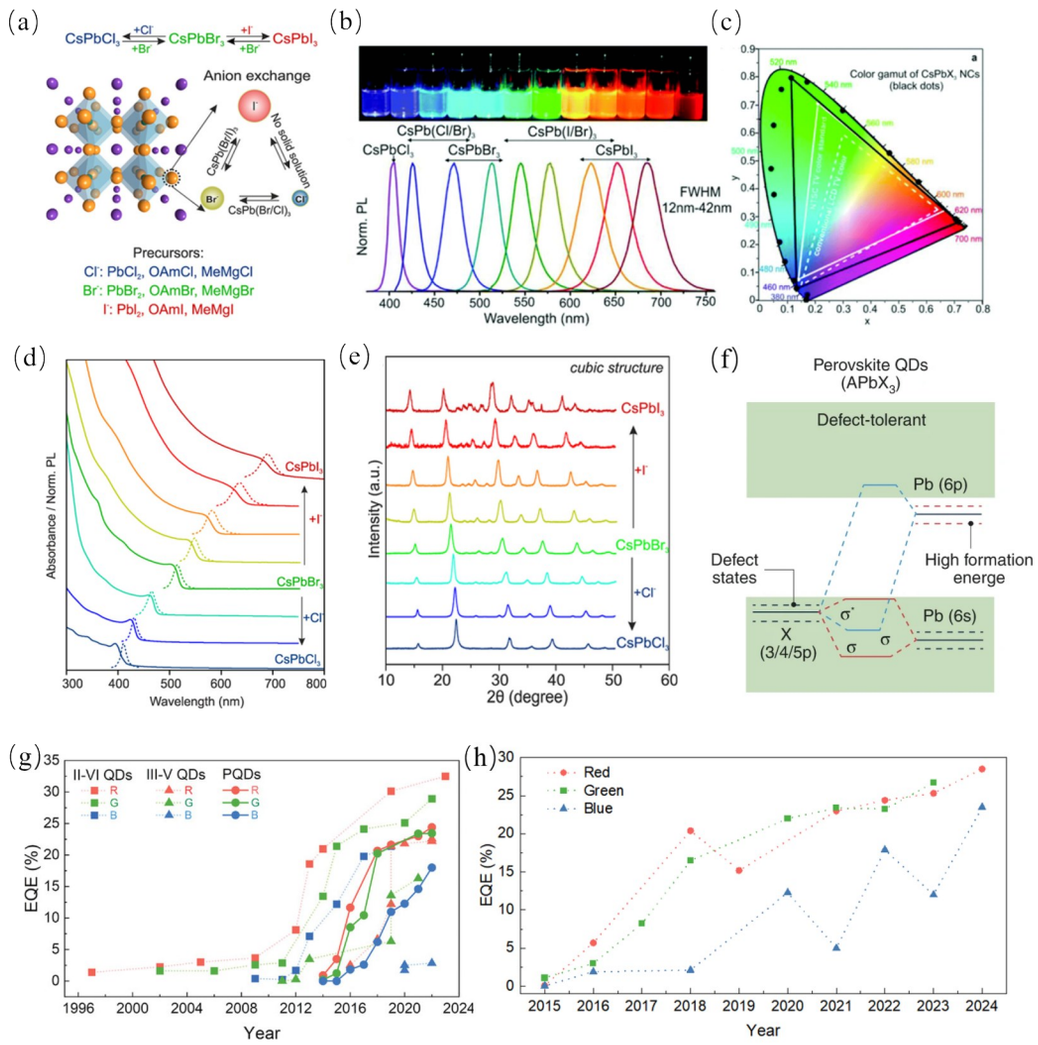

Fig.1 (a) Schematic diagram of anion exchange in the cubic perovskite crystal structure of $CsPbX_3$[16]. (b) Fluorescence spectra and corresponding images of $CsPbX_3$ QDs under UV light, illustrating anion tuning[14]. (c) Comparison of the emission from metal halide perovskite (MHP) QDs (black dots) with the standard gamut for typical LCD TVs (dotted triangle) and the standard for LCD TVs (solid triangle). Reproduced with permission.[14] Copyright 2015, American Chemical Society. (d) Optical absorption (solid line) and PL spectra (dashed line) of $CsPbBr_3$ QDs[16]. (e) Powder X-ray diffraction (XRD) patterns of original $CsPbBr_3$ QDs and anion-exchanged samples (with $PbCl_2$ and PbI_2 as halide sources). Reproduced with permission.[16] Copyright 2015, American Chemical Society. (f) Band structure of PQDs. Reproduced with permission.[13] Copyright 2022, Springer Nature. (g) Development trend of maximum EQE for red, green, and blue QLEDs devices. Reproduced with permission.[15] Copyright 2024, Wiley-VCH. (h) Major advancements in PQDs and PeLEDs.

tion energy, while shallow-level defects are most commonly observed in LHP QDs. These defects are typically harmless to the PL of $CsPbI_3$ but present greater challenges for $CsPbCl_3$, as shown in Fig. 2 (d). Shallow-level defects slow down the mobility of free charge carriers; once captured, these carriers can be thermally re-excited back into the band structure. Conversely, deep-level defects result in non-radiative recombination, significantly reducing carrier lifetimes and thus severely diminishing the radiative efficiency of LEDs[19], as illustrated in Fig. 2(b). Additionally, surface defects may also serve as pathways for halide ion migration, reducing the activation energy for ionic migration, which, in turn, causes the device's EQE to roll off, as shown in Fig. 2(e).

The instability of the buried interface between the charge transport layer and the perovskite emis-

sion layer is a key limitation in Pe-LEDs, hindering carrier transport and recombination. To tackle this issue, a strategy has been proposed to introduce guanidine hydrochloride (GACl) as a bottom passivation layer[20]. The GACl not only passivates point defects at the buried interface but also releases chloride anions that help inhibit ion migration and prevent the formation of halide vacancies. In addition to passivation, GACl improves the phase purity of the 2D layered perovskite structure, boosting crystallinity and optoelectronic performance. This has resulted in an excellent EQE of 6.61% as shown in Fig. 2(f) and has significantly impacted the device's operational lifetime as shown in Fig. 2(g).

Therefore, the defects in PQDs are crucial to their optoelectronic performance and device, and addressing these defects is one of the key challenges we currently face.

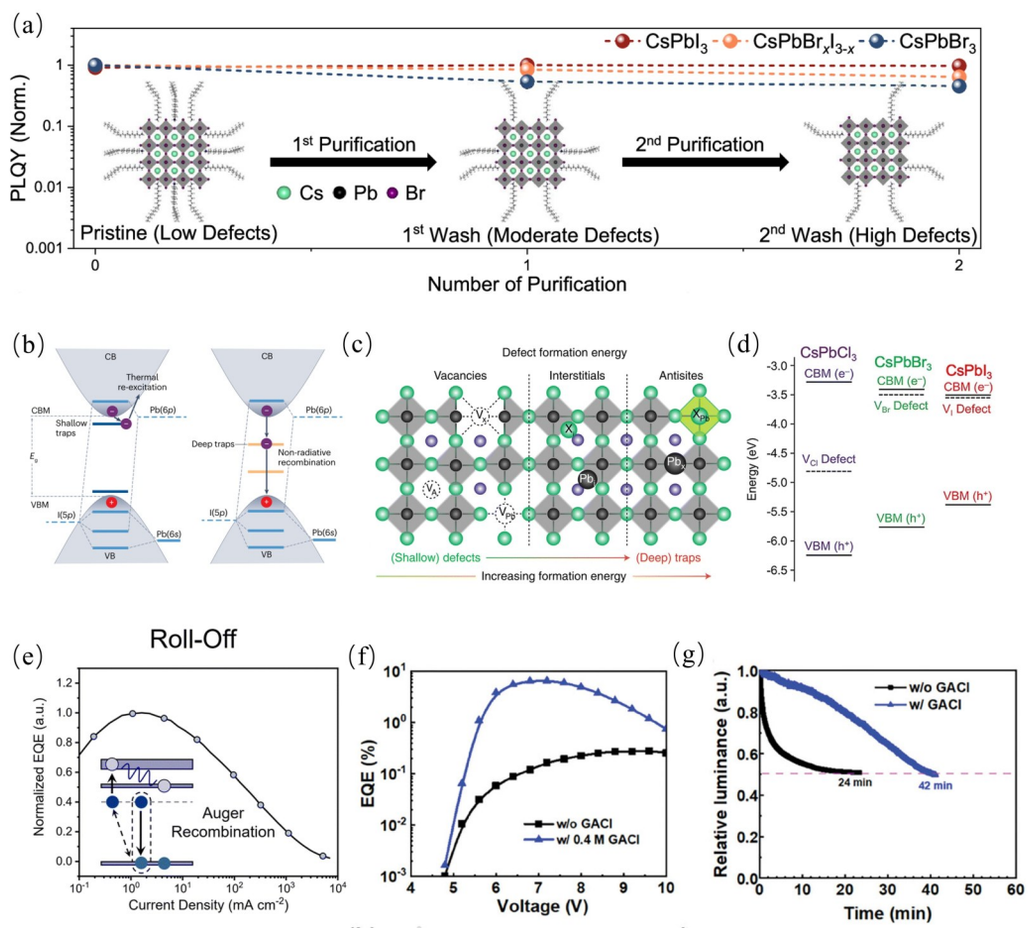

Fig.2 (a) Variation of normalized PLQY for $CsPbI_3$ (red), $CsPbBr_xI_{3-x}$ (orange), and $CsPbBr_3$ (blue) QDs after continuous purification steps. Reproduced with permission.[18] Copyright 2024, Springer Nature. (b) Scheme illustrating deep and shallow-level traps. Reproduced with permission.[19] Copyright 2023, Springer Nature. (c) Typical point defects in LHPs, including vacancies, interstitial atoms, and anti-site atoms, ordered by increasing formation energy and their depths within the bandgap[21]. (d) Transition energy levels of halide vacancies within the bandgap of these materials[21]. (e) Defect-induced ion migration leading to EQE roll-off. Reproduced with permission.[21] Copyright 2023, RSC. (f) EQE curves with corresponding applied biases[20]. (g) Relative brightness decay curves of Pe-LEDs with different underlying GACl concentrations (showing PeLEDs under 6 V). Reproduced with permission.[20] Copyright 2024, Wiley-VCH.

4 Optimization Strategies

4.1 Ligand Engineering

In the study of PQDs, ligand engineering has been proven to be a crucial strategy for enhancing device performance and stability. By selecting appropriate ligands to modify the material surface, it is possible to effectively reduce defect density, sup-

press ion migration, improve carrier mobility, and enhance emission efficiency.

Yasser Hassan et al. synthesized $MAPb(I_xBr_{1-x})_3$ QDs (with MA standing for methylammonium) through an improved ligand-assisted re-precipitation technique and elucidated how the functionality of MHP is highly sensitive to the properties of QD surfaces[22]. Following purification, the nanocrystals were treated with ethylenediaminetetraacetic acid (EDTA) and reduced glutathione (GSH), as shown in Fig. 3(a). These molecules exhibit a strong binding affinity for lead in biological systems, helping to remove uncoordinated lead from the surface of QDs, as illustrated in Fig. 3(b). This ligand treatment creates a "clean" surface, reducing defects, while also being highly effective in suppressing halide segregation and improving bandgap stability[23].

Additionally, as ligands can influence the hole and electron mobility of PQDs[24] as shown in Fig. 3 (c), we can attribute the instability of PQDs to three main factors. First, the acid-base reaction between oleic acid (OA) and oleylamine (OAm) can cause their reversible detachment from the PQD surface, leaving under-coordinated sites. Second, the reaction between OAm and OA forms oleylamide, which induces surface defects and aggregation in PQDs, while also producing H_2O, which can degrade the perovskite. Third, OAm can easily detach from the surface as an oil-based halide ammonium by coordinating with neighboring surface X ions.

Ligand-exchanged PQDs exhibited high mobility and high PLQY, making them suitable for both PL and EL applications. However, due to the decomposition of high-ionic perovskites by polar solvents used for ligand exchange in PQDs, Yi-Tong Dong et al. proposed a method of surface replacement for PQDs, developing a bipolar shell with an inner anionic layer and an outer layer of cationic and polar solvent molecules[25]. Compared to previously reported low-dimensional perovskites, this method produced strongly constrained PQDs solids, increasing carrier mobility ($\geqslant 0.01\ cm^2 \cdot V^{-1} \cdot s^{-1}$), reducing trap density, and allowing for successful exchange and redispersion, as shown in Fig. 3(d). Additionally, the ligand design strategy by Kang Wang et al. demonstrated that increasing the π-conjugation length and increasing the cross-sectional area of the ligands significantly suppresses ionic transport[26], narrows phase distribution, reduces defect density, and enhances radiative recombination efficiency, as shown in Fig. S2(f).

Moreover, in existing studies, the introduction of inorganic ligands is a common approach, but these methods typically depend on highly polar solvents (such as DMF) for inorganic salts, which compromise the structural stability of perovskites and affect the operational performance of LEDs. To better passivate surfaces, our team proposed a strategy to introduce inorganic ligands into the anti-solvent used for reverse purification[27], as shown in Fig. 3(e). This strategy employs an in situ inorganic ligand approach to achieve consistent PL emission spectra, as shown in Fig. 3(f) and maintaines luminescence intensity without extra peaks or emission broadening, effectively improving the optical properties of MHP QDs.

4.2 Self-Assembly Strategy

Self-assembly and regeneration technologies offer a straightforward and efficient "bottom-up" approach that enables MHP nanostructures to rearrange their overall appearance. However, the self-assembly of QDs is typically initiated by solvent evaporation or by changing the polarity of reaction system, which destabilizes the terminating ligands of the QDs.

As shown in Fig. 4(a), nanostructures are assembled through colloidal solvent evaporation[28]. During the solvent evaporation process, the distance between particles decreases, allowing QDs to assemble in an ordered fashion, thereby optimizing the system's entropy. In the QD solution, repulsive forces dominate, favoring monodispersion of the QDs (as shown in Fig. 4(b)[29], dark green trace). However, during self-assembly, effective inter-particle interactions transition from repulsive to attractive (as shown in Fig. 4(b), light green trace). As the solvent is fully removed, the QDs pack tightly and start to form superlattices, at which point the elastic repulsive forc-

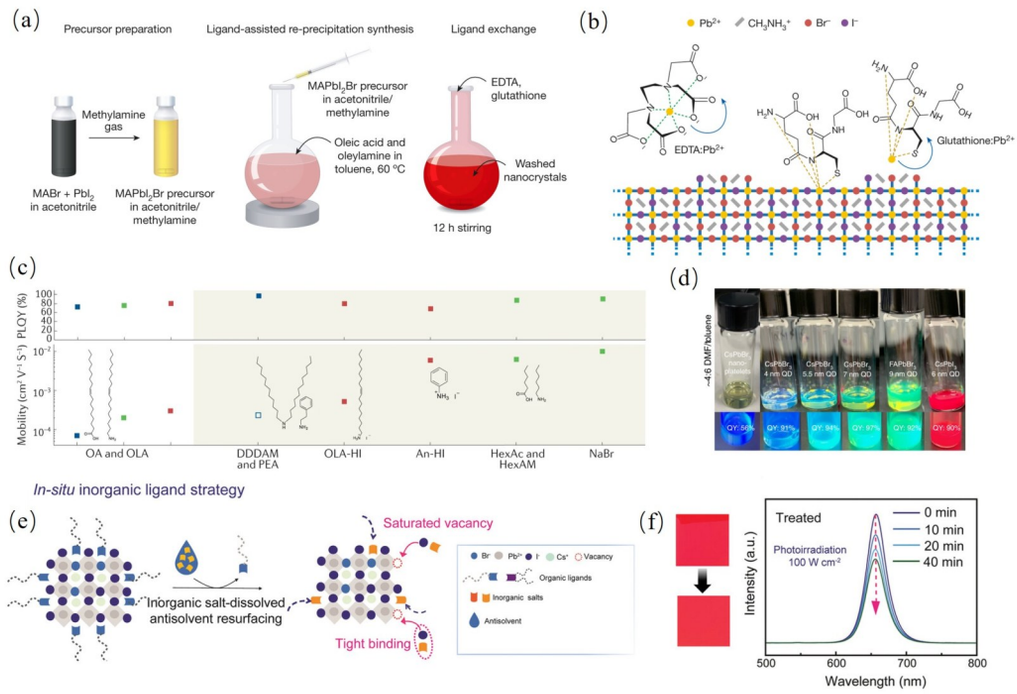

Fig.3 (a) Synthesis and ligand treatment steps: Dissolving perovskite precursors in acetonitrile and methylamine; synthesizing QDs via an improved ligand-assisted reprecipitation method; and applying post-synthesis ligand treatment[22]. (b) Molecular interactions between glutathione, EDTA, and Pb^{2+} atoms on the surface. Reproduced with permission.[22] Copyright 2021, Springer Nature. (c) PLQY and carrier mobility of PQDs with varying ligand compositions. (Solid squares represent hole mobility, while hollow squares represent electron mobility, with each point's color corresponding to the emission color of the respective PQDs. Shaded areas highlight ligands that can replace traditional OA and OAm). Reproduced with permission.[24] Copyright 2022, Springer Nature. (d) Bipolar surface-modified PQDs of different sizes, shapes, and compositions suspended in a DMF/toluene mixture. Reproduced with permission.[25] Copyright 2020, Springer Nature. (e) Process and advantages of using an in situ inorganic ligand strategy with weakly polar anti-solvents[27]. (f) Bandgap stability of treated MHP films under 100 W·cm^{-2} light irradiation. Reproduced with permission.[27] Copyright 2022, Wiley-VCH.

es of the ligands balance with van der Waals (vdW) forces.

Moreover, when the active layer thickness approaches approximately 5 nm, it leads to tunneling and direct electrical interactions between the hole transport layer (HTL) and the electron transport layer (ETL), resulting in unwanted exciton complex emissions in the LED, as shown in Fig. 4(d). Our team identified a bifunctional terminating ligand to modify the polarity of the $CsPbBr_3$ c-QD surface[30]. This strategy not only passivates QD surface defects but also establishes the necessary polarity difference between the HTL and the perovskite. Applied to uniformly sized c-QDs, self-assembly can be achieved while avoiding the dissolution of the HTL substrate, as shown in Fig. 4(c). We demonstrated that clearly defined, ordered, and compact monolayers can suppress HTL/ETL interactions, achieving a current density that is twice as high as that seen in the control, as shown in Fig. 4(e), along with nearly Rec. 2100 primary blue light emission.

The long-range order in PQDs films is typically poor due to variations in dot size, surface ligand density, and inconsistent stacking, all of which hinder carrier injection and lead to poor operational stability. To enhance the long-range order, our team also reported a synergistic dual-ligand strategy[31]. The liquid trimethylsilyl bromide (ETM Br) works well with non-polar solvents and reacts with protonating reagents to produce HBr, which in situ dissolve smaller QDs and connect uniformly sized dots to

achieve coherence from dot to dot. This process also effectively removes low-conductivity ligands, creating dense, uniform, and defect-free films as shown in Fig. 4(f). These films exhibit high electrical conductivity, which enhances the operational stability of LED devices, as shown in Fig. 4(g).

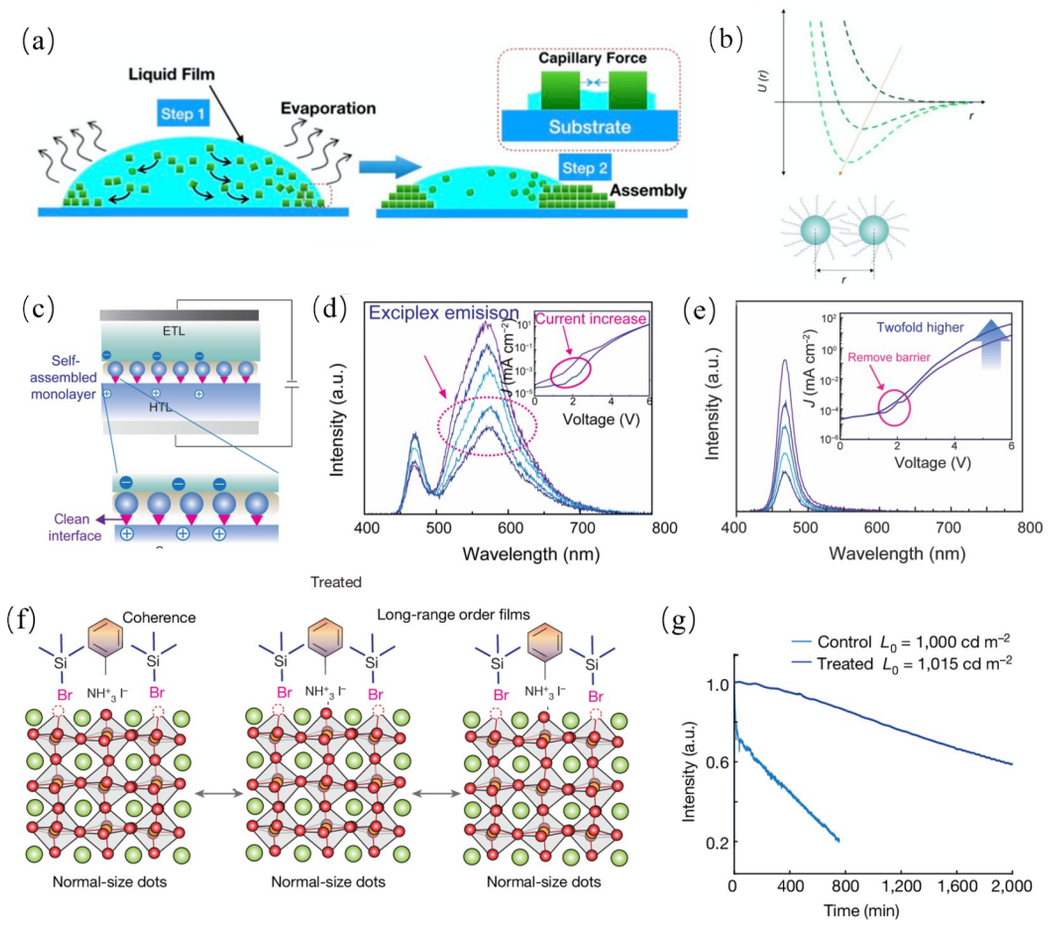

Fig.4 (a) Schematic illustration of capillary forces associated with solvent evaporation. Reproduced with permission.[28] Copyright 2022, American Chemical Society. (b) Changes in the effective pair interaction potential, U, at different stages of self-assembly. Reproduced with permission.[29] Copyright 2016, American Chemical Society. (c) Schematic of the HTL-compatible ligand strategy[30]. (d) EL of monolayer LEDs at various current densities (10 to 40 mA·cm^{-2}). They exhibit a combination of exciton complex and blue light emission. (Inset indicates a reduction in injection barrier for monolayer LEDs)[30]. (e) Monolayer LEDs demonstrate Rec. 2100 color-accurate blue light emission. (Inset shows doubled current density and reduced injection barriers). Reproduced with permission.[30] Copyright 2023, AAAS. (f) Long-range order control strategy[31]. (g) Operating stability of control and treated LEDs. Reproduced with permission.[31] Copyright 2024, Springer Nature.

5 Conclusion and Outlook

Achieving efficient and stable emission in PQDs devices has faced several challenges, such as interface defects, charge carrier injection imbalance, and poor long-range ordering of QD films. Through ligand engineering, interface passivation, and self-assembly strategies, researchers have developed effective solutions.

To address the instability of PQDs, isolating them from the external environment can significantly enhance the stability of Pe-QLEDs. In this context, adopting a core/shell structure is a promising strategy[32-33]. When designing an appropriate shell for blue PQDs, several critical characteristics must be considered. The ideal shell material should provide

good lattice matching, excellent surface passivation, superior optoelectronic properties (such as a wide bandgap), and strong chemical and environmental stability. Moreover, most PQDs, particularly blue PQDs, exhibit a deep valence band maximum (VBM), resulting in significant hole-injection barriers between QDs and HTLs, which in turn leads to carrier imbalance in Pe-QLEDs and decreases the efficiency and stability. Developing new HTLs which have a better energy alignment with the emitting layer or modulating the energy level of the HTL through doping are promising ways to balance electron and hole injection[34-35], thereby enhancing radiative recombination efficiency.

Pe-LEDs have tremendous potential in future display technologies, which not only raises performance requirements for visible light sources but also for other wavelengths, such as near infrared and mid infrared. Because of the native bandgap limit, there are only $FAPbI_3$ QDs and Sn-based QDs can realize the band-edge NIR emission. limited by band gap, $FAPbI_3$ can only realized emission near 800 nm and can not satisfy the longer emission wavelength[36]. Although the Sn-based QDs can realize the NIR emission up to 950 nm, the large ratio of surface-to-volume of the Tin PQDs leads to massive surface defects, making the low PLQY (<0.2%). There is another way to realize NIR emission for PQDs. Because of the halide perovskites are ideal sensitizing host materials as they exhibit large absorption coefficients and ionic nature, which make them the ideal host matrix for rare earth elements. Through doping the rare earth elements like Yb^{4+}[37-38], PQDs can realize the NIR emission (1000 nm) with 200% PLQY comes from 4f-4f transitions of Yb^{3+} ions and quantum cutting effect. However, these high Yb^{3+} alloyed materials show inferior stability and PLQY drop due to the Yb^{3+} induced precipitation in ambient conditions, limiting their application in NIR-LEDs. Therefore, how to achieve efficient energy transfer and use other rare earth ions to achieve longer emission wavelengths is what we need to focus on.

References:

[1] HUANG C Y, LI H C, WU Y, *et al*. Inorganic halide perovskite quantum dots: A versatile nanomaterial platform for electronic applications [J]. *Nano-Micro Lett.*, 2023, 15(1): 16.

[2] 曾海波,董宇辉. 钙钛矿量子点:机遇与挑战 [J]. 发光学报, 2020, 41(8): 940-944.
ZENG H B, DONG Y H. Perovskite quantum dots: opportunities and challenges [J]. *Chin. J. Lumin.*, 2020, 41(8): 940-944.

[3] EKIMOV A I, ONUSHCHENKO A A. Quantum size effect in three-dimensional microscopic semiconductor crystals [J]. *JETP Lett.*, 2023, 118(S1): S15-S17.

[4] ROSSETTI R, BRUS L. Electron-hole recombination emission as a probe of surface chemistry in aqueous cadmium sulfide colloids [J]. *J. Phys. Chem.*, 1982, 86: 4470-4472.

[5] MURRAY C B, NORRIS D J, BAWENDI M G. Synthesis and characterization of nearly monodisperse CdE (E = sulfur, selenium, tellurium) semiconductor nanocrystallites [J]. *J. Am. Chem. Soc.*, 1993, 115(19): 8706-8715.

[6] ZHANG Y M, LI Y Y, LIU Y Z, *et al*. Quantum confinement luminescence of trigonal cesium lead bromide quantum dots [J]. *Appl. Surf. Sci.*, 2019, 466: 119-125.

[7] ZHANG J B, LIU X F, JIANG P F, *et al*. Red-emitting $CsPbBrI_2$/PbSe heterojunction nanocrystals with high luminescent efficiency and stability for bright light-emitting diodes [J]. *Nano Energy*, 2019, 66: 104142.

[8] SHIRASAKI Y, SUPRAN G J, BAWENDI M G, *et al*. Emergence of colloidal quantum-dot light-emitting technologies [J]. *Nat. Photonics*, 2013, 7(1): 13-23.

[9] KONG L M, SUN Y Q, ZHAO B, *et al*. Fabrication of red-emitting perovskite LEDs by stabilizing their octahedral structure [J]. *Nature*, 2024, 631(8019): 73-79.

[10] 刘王宇, 陈斐, 孔淑祺, 等. 全无机钙钛矿量子点的合成、性质及发光二极管应用进展 [J]. 发光学报, 2020, 41(2): 117-133.
LIU W Y, CHEN F, KONG S Q, *et al*. Synthesis, properties and application of all-inorganic perovskite quantum dots [J].

Chin. J. Lumin., 2020, 41(2): 117-133.

[11] 邓艳红, 朱莹, 陈默, 等. 红光钙钛矿发光二极管研究进展[J]. 发光学报, 2024, 45(10): 1683-1698.
DENG Y H, ZHU Y, CHEN M, *et al.* Research progress of red perovskite light-emitting diodes [J]. *Chin. J. Lumin.*, 2024, 45(10): 1683-1698.

[12] 卜世啸, 葛子义. 钙钛矿发光二极管的研究进展[J]. 液晶与显示, 2021, 36(1): 105-112.
BU S X, GE Z Y. Research progress of perovskite light-emitting diodes [J]. *Chin. J. Liq. Cryst. Disp.*, 2021, 36(1): 105-112.

[13] BUCKLEY A K, MA S, HUO Z, *et al.* Nanomaterials for carbon dioxide conversion at industrial scale [J]. *Nat. Nanotechnol.*, 2022, 17(8): 811-813.

[14] PROTESESCU L, YAKUNIN S, BODNARCHUK M I, *et al.* Nanocrystals of cesium lead halide perovskites ($CsPbX_3$, X = Cl, Br, and I): Novel optoelectronic materials showing bright emission with wide color gamut [J]. *Nano Lett.*, 2015, 15(6): 3692-3696.

[15] SHAN Q S, DONG Y H, XIANG H Y, *et al.* Perovskite quantum dots for the next-generation displays: Progress and prospect [J]. *Adv. Funct. Mater.*, 2024: 2401284.

[16] NEDELCU G, PROTESESCU L, YAKUNIN S, *et al.* Fast anion-exchange in highly luminescent nanocrystals of cesium lead halide perovskites ($CsPbX_3$, X = Cl, Br, I) [J]. *Nano Lett.*, 2015, 15(8): 5635-5640.

[17] YANG W M, ZHANG B, ZHANG Q T, *et al.* Adjusting the band structure and defects of ZnO quantum dots via tin doping [J]. *RSC Adv.*, 2017, 7(19): 11345-11354.

[18] YE J Z. Extending the defect tolerance of halide perovskite nanocrystals to hot carrier cooling dynamics [J]. *Nat. Commun.*, 2024, 15: 8120.

[19] ZHANG H, PFEIFER L, ZAKEERUDDIN S M, *et al.* Tailoring passivators for highly efficient and stable perovskite solar cells [J]. *Nat. Rev. Chem.*, 2023, 7(9): 632-652.

[20] DO J J, JUNG J W. Strategic buried defect passivation of perovskite emitting layers by guanidinium chloride for high-performance pure blue perovskite light emitting diodes [J]. *Small*, 2024: 2400544.

[21] YANG J N, WANG J J, YIN Y C, *et al.* Mitigating halide ion migration by resurfacing lead halide perovskite nanocrystals for stable light-emitting diodes [J]. *Chem. Soc. Rev.*, 2023, 52(16): 5516-5540.

[22] HASSAN HASSAN Y. Ligand-engineered bandgap stability in mixed-halide perovskite LEDs [J]. *J. Phys. Chem. C*, 2021, 125(43): 23968-23975.

[23] DU FOSSÉ I, LAL S, HOSSAINI A N, *et al.* Effect of ligands and solvents on the stability of electron charged CdSe colloidal quantum dots [J]. *J. Phys. Chem. C*, 2021, 125(43): 23968-23975.

[24] HAN T H, JANG K Y, DONG Y, *et al.* A roadmap for the commercialization of perovskite light emitters [J]. *Nat. Rev. Mater.*, 2022, 7(10): 757-777.

[25] DONG Y T, WANG Y K, YUAN F L, *et al.* Bipolar-shell resurfacing for blue LEDs based on strongly confined perovskite quantum dots [J]. *Nat. Nanotechnol.*, 2020, 15(8): 668-674.

[26] WANG K, LIN Z Y, ZHANG Z H, *et al.* Suppressing phase disproportionation in quasi-2D perovskite light-emitting diodes [J]. *Nat. Commun.*, 2023, 14(1): 397.

[27] WANG Y K, SINGH K, LI J Y, *et al.* In situ inorganic ligand replenishment enables bandgap stability in mixed-halide perovskite quantum dot solids [J]. *Adv. Mater.*, 2022, 34(21): 2200854.

[28] LIU J, ZHENG X, MOHAMMED O F, *et al.* Self-assembly and regrowth of metal halide perovskite nanocrystals for optoelectronic applications [J]. *Acc. Chem. Res.*, 2022, 55(3): 262-274.

[29] BOLES M A, ENGEL M, TALAPIN D V. Self-assembly of colloidal nanocrystals: From intricate structures to functional materials [J]. *Chem. Rev.*, 2016, 116(18): 11220-11289.

[30] WANG Y K, JIA F Y, LI X Y, *et al.* Self-assembled monolayer – based blue perovskite LEDs [J]. *Sci. Adv.*, 2023, 9(36): eadh2140.

[31] WANG Y K, WAN H Y, TEALE S, *et al.* Long-range order enabled stability in quantum dot light-emitting diodes [J]. *Nature*, 2024, 629(8012): 586-591.

[32] KIM J S, HEO J M, PARK G S, *et al.* Ultra-bright, efficient and stable perovskite light-emitting diodes [J]. *Nature*, 2022, 611(7937): 688-694.

[33] DONG Y T, WANG Y K, YUAN F L, *et al*. Bipolar-shell resurfacing for blue LEDs based on strongly confined perovskite quantum dots [J]. *Nat. Nanotechnol.*, 2020, 15(8): 668-674.

[34] NONG Y Y, YAO J S, LI J Q, *et al*. Boosting external quantum efficiency of blue perovskite QLEDs exceeding 23% by trifluoroacetate passivation and mixed hole transportation design [J]. *Adv. Mater.*, 2024, 36(27): 2402325.

[35] NONG Y Y, YAO J S, LI J Q, *et al*. Gradient hole injection inducing efficient exciton recombination in blue (475 nm) perovskite QLEDs [J]. *Nano Lett.*, 2024: acs. nanolett. 4c02600.

[36] TSENG Z L, CHEN L C, CHAO L W, *et al*. Aggregation control, surface passivation, and optimization of device structure toward near-infrared perovskite quantum-dot light-emitting diodes with an EQE up to 15. 4% [J]. *Adv. Mater.*, 2022, 34(18): 2109785.

[37] YU Y J, WANG H S, PAN J L, *et al*. Monovalent charge compensation enables efficient lanthanide-based near-infrared perovskite LEDs [J]. *Adv. Funct. Mater.*, 2023, 33(45): 2305125.

[38] YU Y J, ZOU C, SHEN W S, *et al*. Efficient near-infrared electroluminescence from lanthanide-doped perovskite quantum cutters [J]. *Angew. Chem. Int. Ed.*, 2023, 62(22): e202302005.

李梦娇(2002-),女,硕士研究生,2024年于济南大学获得学士学位,主要从事量子点发光材料与器件的研究。
E-mail: 20244214064@stu. suda. edu. cn

王亚坤(1990-),男,博士,副教授,2020年12月获苏州大学博士学位,2018-2020年在加拿大多伦多大学Edward H. Sargent教授课题组联合培养,随后在苏州大学和多伦多大学进行博士后研究,主要从事有机光电功能材料的设计、合成、表征与其在光电转换器件中的应用,纳米材料的合成与其在光电转换器件中的应用,新型半导体材料在短波红外和中波红外区域实现高性能发光器件的研究。
E-mail: wangyakun@suda. edu. cn